

Hydrogen production from methane conversion in a gliding arc

Mariano Garduño^{2,1}, Marquidia Pacheco^{1,4}, Joel Pacheco^{1,2}, Ricardo Valdivia^{1,2}, Alfredo Santana^{3,4}, Benoîte Lefort⁴, Nadia Estrada^{2,1}, Carlos Rivera^{1,2},

¹Instituto Nacional de Investigaciones Nucleares Carretera México-Toluca s/n, La Marquesa, Ocoyoacac, Estado de México, C. P. 52750, México. marquidia.pacheco@inin.gob.mx

²Instituto Tecnológico de Toluca Av. Instituto Tecnológico s/n, Ex-Rancho la Virgen, Metepec, Estado de México, C. P. 52140, México.

³Instituto Tecnológico y de Estudios Superiores de Monterrey Campus Toluca Eduardo Monroy Cárdenas #2000, San Antonio Buenavista, Toluca, México

⁴Institut Supérieur de l'Automobile et des Transports 49 Rue Demoiselle Bourgeois Nevers, 58000, France.

Abstract

Until now the major problem of the methane conversion is to break the very strong C-H bond. It is possible by employing some catalysts methods, however the formation of carbon powder diminish the catalytic performance.

The use of a gliding arc described in this work has a double goal: the hydrogen production and other syngas like acetylene and the treatment of the green house gas methane without no performance diminution whit carbonaceous products formed.

A good approximation model describing the chemical processes concerning the methane decomposition is described, first by the interaction of key radicals like CH₃ and H, and after by chemical reactions involving other hydrocarbons.

Additionally, the experimental results demonstrated the ability of the gliding arc to accelerate chemical reactions at low temperatures and at low energetic costs.

Keywords: hydrogen production, gliding arc, methane, syngas

1. Introduction

Because of its greenhouse effect, many studies on methane conversion into more valuable compounds [1], such as hydrogen, synthesis gas or even carbon nanostructures synthesis [2, 3] have been studied.

In general, catalytic methods overcome to break the strong bond characteristic of methane, nevertheless the carbonaceous powder obtained diminish the catalytic effect [4,5].

Nowadays, investigations have been deeply performed using non-conventional technology, like plasma technology. Nonthermal plasmas are widely studied for methane conversion [5-17]. These techniques are cheap and easy to handle; but, the main problem is their low plasma density and subsequently the difficult to achieve higher conversion at higher flow rate.

On the other side, thermal plasmas which typically high temperature and higher density of plasma [3, 18-22] are capable to maintain elevated injection of gas; however the instrument cost is expensive and they spend higher power consumption.

Therefore, a plasma device combining the better characteristics of nonthermal and thermal plasmas mentioned before, becomes interesting. The gliding arc plasma has a transition region, allowing higher electron density, higher temperatures and it is capable to treat higher

injection flow rates, therefore this kind of devices have greater possibilities to be applied in industry [23-26].

In the present paper a model describing the chemical processes concerning the methane decomposition is proposed and, concerning the experimental part, the ability of the gliding arc to accelerate chemical reactions at low temperatures and at low energetic costs is demonstrated.

2. Theory of chemical kinetic model

The energetic electrons transfer their energy toward neutral molecules of the polluted gas resulting in quenching, attachment, dissociation, or ionization process; species like free radicals, metastables, atoms and ions are also formed. In particular, in the proposed kinetic model, the radicals are initially formed and the synthesis of hydrogen and other hydrocarbons are finally formed.

In total 24 chemical species (e , Ar , Ar^* - Ar metastable, CH_4 , CH , H , H_2 , CH_2 , CH_3 , H^+ , CH^* , H^* , C_2H_6 , C_2H_5 , C_3H_X , C_2H_4 , C_4H_X , CH_4^+ , CH_3^+ , $C_2H_4^+$, $C_2H_5^+$, $C_3H_X^+$, CH_5^+ , $C_4H_X^+$ with $X>5$) and 43 chemical reactions were considered.

Specifically, the chemical kinetic model employed involves reactions with excited argon having a non negligible role [27] in the plasma chemistry during the methane decomposition (table 1):

Table 1. Excited argon reactions

	<i>Reaction</i>	<i>Rate constant,</i> <i>cm³/s</i>	<i>Reference</i>
1	$e + Ar \rightarrow e + Ar^*$	$8 \times 10^{-9}, f(E/n)$	[28,29]■
2	$Ar^* + CH_4 \rightarrow Ar + CH_2 + 2H$	5.8×10^{-11}	[27]
3	$Ar^* + CH_4 \rightarrow Ar + CH + H + H_2$	5.8×10^{-11}	[27]
4	$Ar^* + CH_4 \rightarrow Ar + CH_3 + H$	5.8×10^{-11}	[27]
5	$Ar^* + Ar^* \rightarrow Ar^+ + Ar + e$	6.2×10^{-10}	[30,31]
6	$Ar^* + Ar \rightarrow 2Ar$	3.0×10^{-15}	[30,31]

■ Rate constant depending of the reduced electric field E/n (n is the gas number density) calculated by [28], following the energy-level diagram at 13.4eV [29]

Other reactions are also employed, like electron impact reactions, neutral-neutral reactions and ion molecule reactions, as shown in table 2.

Table 2. Reactions and rate coefficients

	<i>Reaction</i>	<i>Rate constant, cm³/s</i>	<i>Reference</i>
	<i>Electron impact</i>		
7	$e + CH_4 \rightarrow CH_3 + H + e$	4.5×10^{-8}	[32]
8	$e + CH_4 \rightarrow CH_2 + H_2 + e$	7.3×10^{-9}	[32]
9	$e + CH_4 \rightarrow CH + H_2 + H + e$	3.7×10^{-9}	[32]
10	$e + CH_4 \rightarrow CH^* + H_2 + H + e$	4.0×10^{-10}	[32]
11	$e + CH_4 \rightarrow CH_3 + H^* + e$	0.8×10^{-10}	[32]
12	$e + C_2H_6 \rightarrow C_2H_5 + H + e$	1.7×10^{-7}	[32]
13	$e + C_3H_x \rightarrow C_2H_4 + CH_4 + e$	2.3×10^{-7}	[32]
14	$e + C_4H_x \rightarrow C_3H_x + CH_4 + e$	2.8×10^{-7}	[32]
15	$e + H_2 \rightarrow H + H + e$	0.2×10^{-7}	[32]
16	$e + CH_4 \rightarrow CH_4^+ + 2e$	3.4×10^{-8}	[32]
17	$e + CH_4 \rightarrow CH_3^+ + H + 2e$	3.2×10^{-8}	[32]
18	$e + C_2H_4 \rightarrow C_2H_4^+ + 2e$	3.0×10^{-7}	[32]
19	$e + C_2H_6 \rightarrow C_2H_4^+ + H_2 + 2e$	3.0×10^{-7}	[32]
20	$e + C_3H_x \rightarrow C_2H_5^+ + CH_3 + 2e$	4.0×10^{-7}	[32]
21	$e + C_4H_x \rightarrow C_3H_x^+ + CH_3 + 2e$	5.0×10^{-7}	[32]
	<i>Neutral-neutral</i>		
22	$CH_3 + CH_3 \rightarrow C_2H_6$	3.7×10^{-11}	[32]
23	$CH_3 + CH_3 \rightarrow C_2H_5 + H$	4.88×10^{-9}	[33]
24	$C_2H_5 + H \rightarrow C_2H_4 + H_2$	5.85×10^{-21}	[33]
25	$CH_3 + H \rightarrow CH_2 + H_2$	0.21	[33]
26	$CH_3 + H \rightarrow CH_4$	0.7×10^{-11}	[32]
27	$C_2H_5 + H \rightarrow CH_3 + CH_3$	0.6×10^{-10}	[32]
28	$C_2H_5 + CH_3 \rightarrow C_3H_x$	4.2×10^{-11}	[32]
29	$C_2H_4 + H \rightarrow C_2H_5$	2.8×10^{-13}	[32]
30	$CH_2 + H \rightarrow CH + H_2$	2.7×10^{-10}	[32]
31	$CH + CH_4 \rightarrow C_2H_5$	1.0×10^{-10}	[32]
32	$CH + C_2H_4 \rightarrow C_3H_x$	2.0×10^{-10}	[32]
33	$CH + C_2H_6 \rightarrow C_3H_x$	4.0×10^{-10}	[32]
34	$CH + C_3H_x \rightarrow C_4H_x$	3.0×10^{-10}	[32]
35	$H + H \rightarrow H_2$	1.0×10^{-15}	[32]

Table 2. Reactions and rate coefficients (continued)

	<i>Reaction</i>	<i>Rate constant,</i> <i>cm³/s</i>	<i>Reference</i>
	<i>Ion-molecule</i>		
36	$CH_4^+ + CH_4 \rightarrow CH_5^+ + CH_3$	1.5×10^{-9}	[32]
37	$CH_3^+ + CH_4 \rightarrow C_2H_5^+ + H_2$	1.2×10^{-9}	[32]
38	$CH_5^+ + C_2H_6 \rightarrow C_2H_5^+ + H_2 + CH_4$	5.0×10^{-10}	[32]
39	$C_2H_4^+ + C_2H_4 \rightarrow C_4H_x^+$	4.3×10^{-10}	[32]
40	$C_2H_4^+ + C_2H_6 \rightarrow C_3H_x^+$	1.3×10^{-11}	[32]
41	$C_2H_5^+ + C_2H_4 \rightarrow C_3H_x^+ + CH_4$	3.1×10^{-10}	[32]
42	$C_2H_5^+ + C_2H_4 \rightarrow C_4H_x^+$	3.03×10^{-10}	[32]
43	$C_2H_5^+ + C_2H_6 \rightarrow C_4H_x^+ + H_2$	0.1×10^{-10}	[32]

3. Experimental Setup

Methane and argon are mixed before their introduction to the three phase gliding arc reactor (figure 1). An optical emission spectroscopy study was done with an Ocean Optic ® spectrometer in order to observe some lines and bands of species formed. Mass spectrometry (Cirrus) was also employed to observe products formed.



Figure 1: Experimental reactor

The alternating current supply, depicted in figure 2, is based in a half bridge inverter, the resonant circuit load has a step-up transformer 1:12, in series with a capacitor $C_1=110\text{nF}$, this circuit has an operating frequency at 23.4kHz, high voltages up to 5kVpp can be obtained.

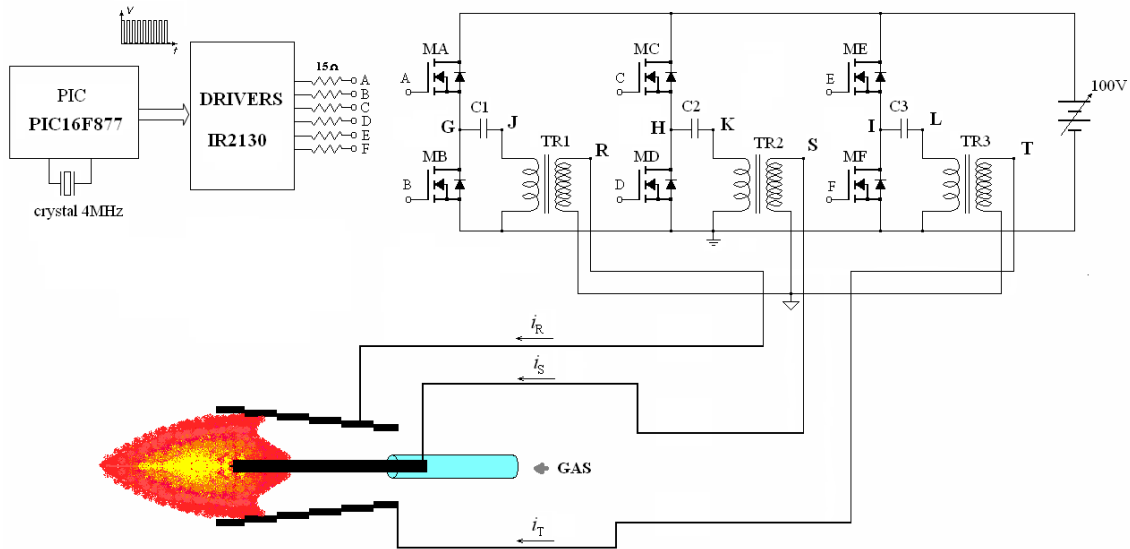


Figure 2. Triphasic alternating current supply

4. Results

4.1 Chemical Model

The evolution of species formed in the plasma reactor can be appreciated in figure 3. The CH_4 diminish quasi instantaneously (time $< 1 \times 10^{-6}$) and the major product formed is composed by H_2 and hydrocarbons with $x > 5$. The acetylene (C_2H_4) is formed but at very low concentrations. Results reported in [32] explain a quasi static evolution in the diminution of methane contrary than results here presented. This could be explained by the introduction of argon in the model having a very important role in the formation of metastable argon acting in the CH_4 decomposition. However it is worth to note that the model reported in [32] is based in a more complete model, a plug flow-rate one.

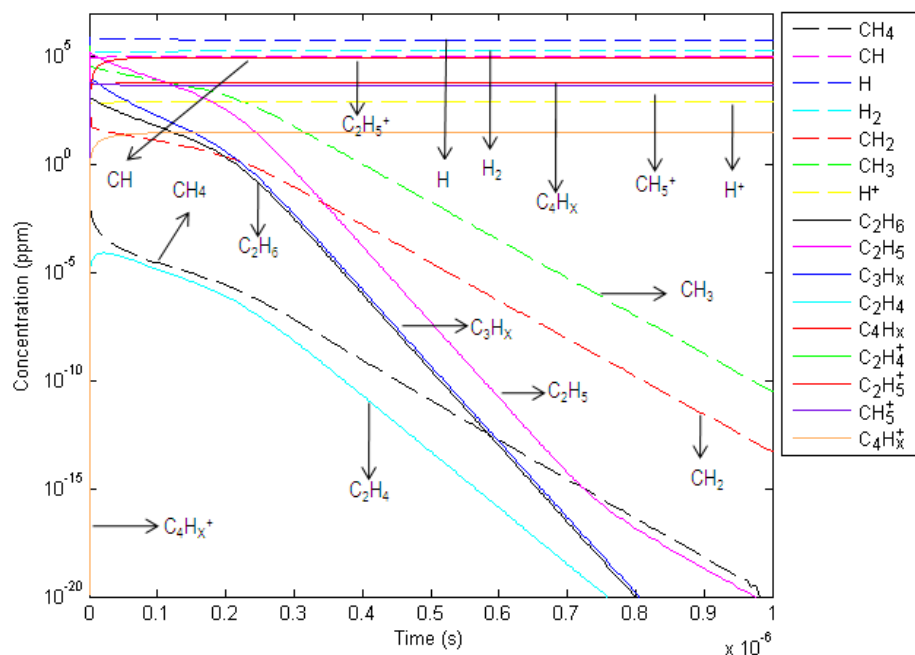


Figure 3. Time evolution of chemical species density

4.2 Electrical analysis

In figure 4, voltage, current and power in line S are illustrated. Small values of these electrical parameters correspond to the initiation of an arc of plasma (i.e situated at the gases entry, where the electrodes are closest). The electric parameters augment in a linear way as the electrodes diverges.

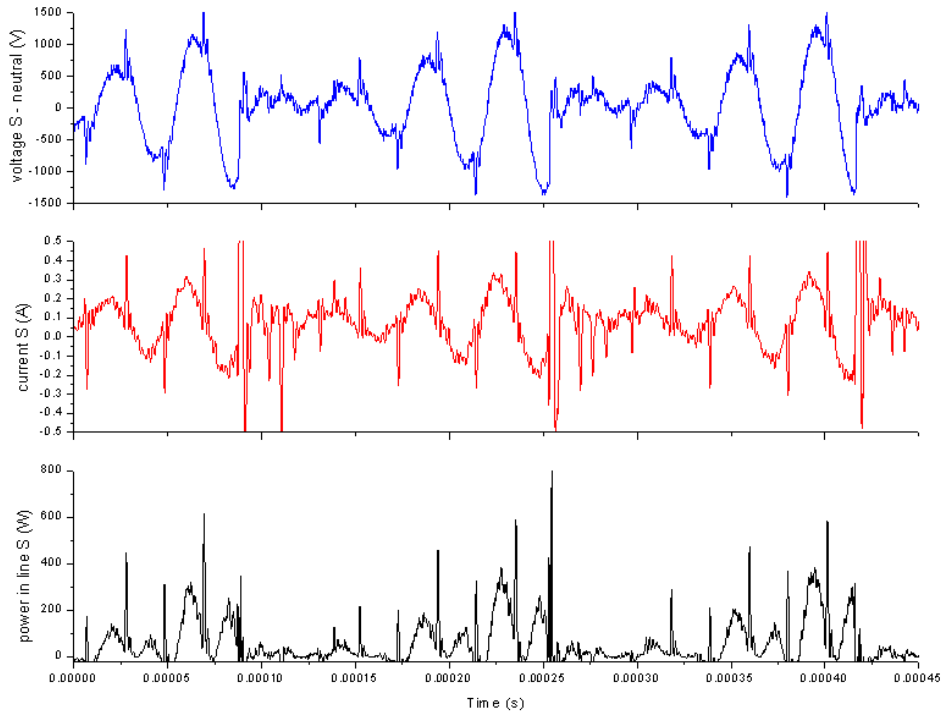


Figure 4. Electrical parameters in line S.

The RMS power obtained from power plotted in figure 4, is depicted by figure 5, where the stabilization of power turns around 248W approximately. Taking into account that the input power was 324W the electrical efficiency is about 76%. The electric loss can be explained by the fact of an elevated number of semiconductors and switching devices.

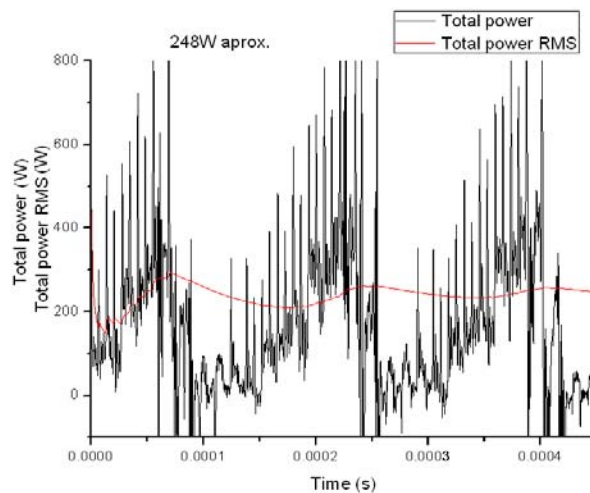


Figure 5. Total power and power RMS

4.3 OES analysis

OES analysis was realized in argon plasma and in a CH₄-argon plasma (figure 6). When methane is introduced, the optical spectrum becomes very rich in carbon bands indicating the CH₄ dissociation. Concerning the H₂ synthesis, in figure 7 the pick situated at 656.3nm [34] indicates its presence when methane is introduced to the plasma.

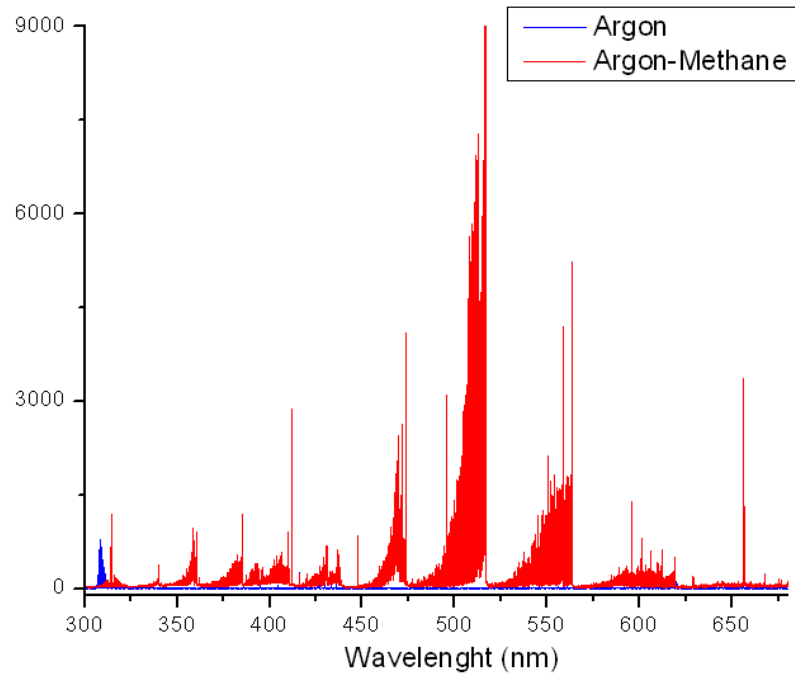


Figure 6. Spectrum of argon plasma and methane-argon plasma

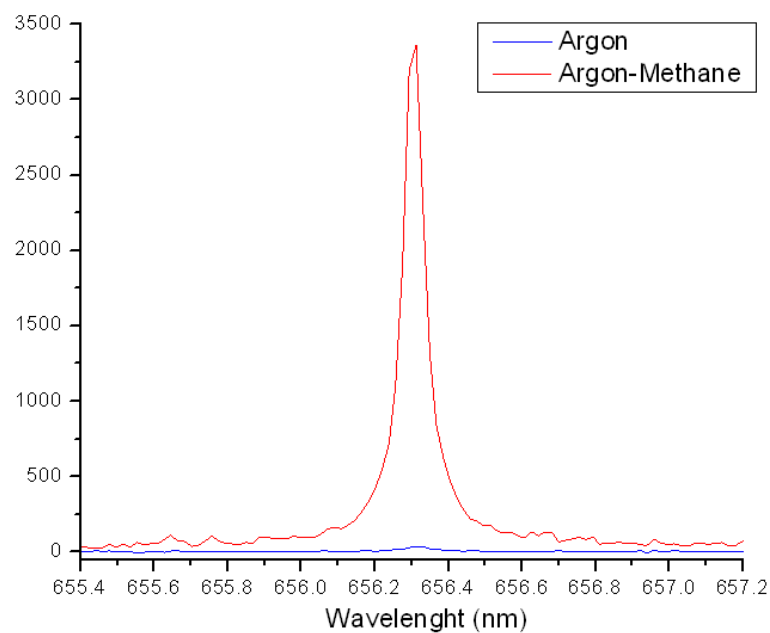


Figure 7. Spectrum of argon plasma and methane-argon at wavelength characteristic of H₂.

4.4 Mass spectrometry analysis

The mass spectra of the gases measured at the outlet of the plasma reactor for argon plasma and when methane is introduced are respectively showed in figures 8 and 9.

As can be appreciated, H_2 , is produced (figure 9) from the decomposition of methane. However, a quantitative analysis was not possible by the fact that other chemical species like hydrocarbons are superposed to oxygen and nitrogen lines obtained in pure argon plasma.

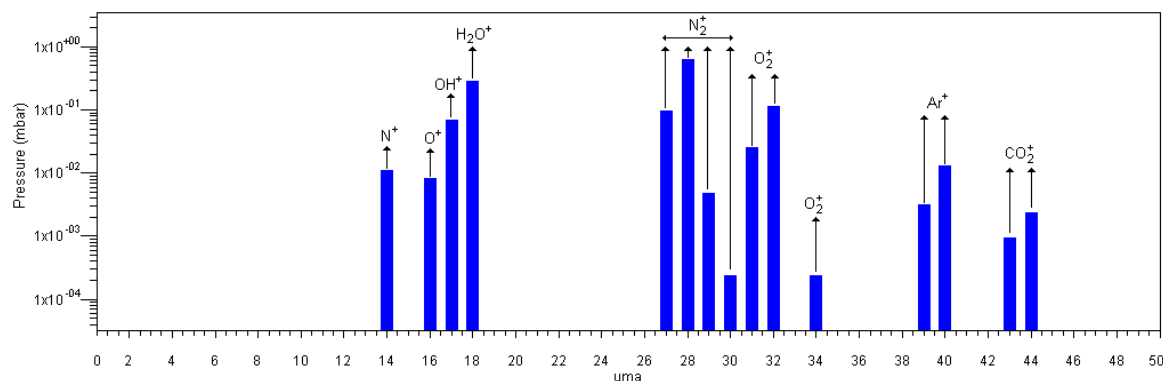


Figure 8. Mass spectrometry of gases obtained from argon plasma.

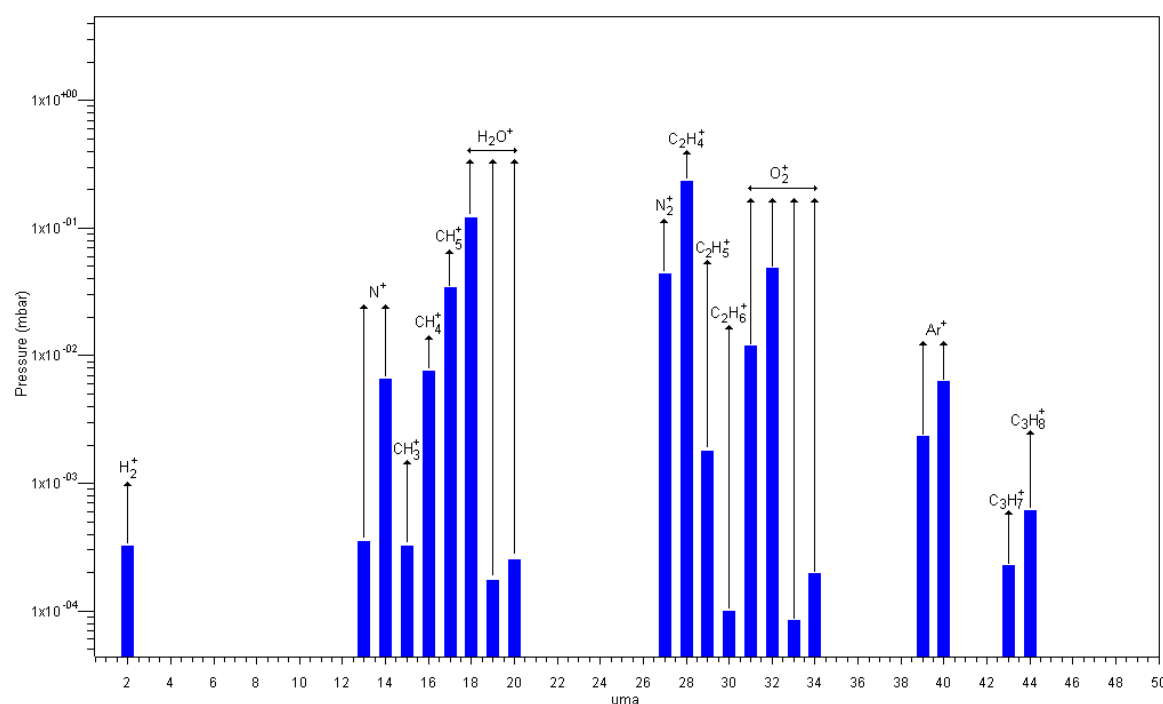


Figure 9. Mass spectrometry of gases obtained from argon-methane plasma.

5. Conclusion

Hydrogen can be obtained from the degradation of methane by a glow discharge, highlighting the important role of argon metastable in this process. It is worth to note that additional experiments have to be done to quantitatively determine the production of hydrogen and other hydrocarbons and to be able to correlate experimental results to model analysis.

6. Acknowledgments:

Project AM810 ININ, L'Oréal-UNESCO-AMC for women in science: To M.Duran, F. Ramos, M. Hidalgo, M. García, R. García for technical support.

REFERENCES

- [1] Shakeel Ahmed, Abdullah Aitani , Faizur Rahman, Ali Al-Dawood, Fahad Al-Muhaish Decomposition of hydrocarbons to hydrogen and carbon Applied Catalysis A: General 359 (2009) 1–24
- [2] A.E. Belikov , V.A. Mal'tsev , O.A. Nerushev, S.A Novopashin, S.Z Sakhapov, D.V Smovzh, Methane Conversion into Hydrogen and Carbon Nanostructures, J. of Eng. Thermophysics 19, (2010) 23-30.
- [3] S.I. Choi, J.S. Nam, J.I. Kim, T.H. Hwang, J.H. Seo, S.H. Hong, Continuous process of carbon nanotubes synthesis by decomposition of methane using an arc-jet plasma, Thin Solid Films 506– 507 (2006) 244 – 249
- [4] Jack H. Lunsford_ Catalytic conversion of methane to more useful chemicals and fuels: a challenge for the 21st century, Catalysis Today 63 (2000) 165–174
- [5] X. Wei, L. Ye, Y. Yuan, Low temperature catalytic conversion of methane to formic acid by simple vanadium compound with use of H₂O₂, Journal of Natural Gas Chemistry 18(2009) 295–299
- [6] J. Luche, O. Aubry, A. Khacef, J.Cormier, Syngas production from methane oxidation using a non-thermal plasma: Experiments and kinetic modeling, Chem. Eng. J. 149 (2009) 35–41
- [7] X.S. Lia, A. Zhua, K.J. Wanga, Y. Xua, Z.M. Song, Methane conversion to C₂ hydrocarbons and hydrogen in atmospheric non-thermal plasmas generated by different electric discharge techniques, Cat. Today 98 (2004) 617–624.
- [8] V. Goujard, J.M. Tatibouet, C. Batiot-Dupeyrat, Use of a non-thermal plasma for the production of synthesis gas from biogas, Appl. Cat.A: General 353 (2009) 228–235.
- [9] Pedro Patiño, Y. Pérez, M. Caetano, Coupling and reforming of methane by means of low pressure radio-frequency plasmas, Fuel 84 (2005) 2008–2014.
- [10] A. Indarto, N. Coowanitwong, J.W. Choia, H. Leea, H. Keun Songa, Kinetic modeling of plasma methane conversion in a dielectric barrier discharge, Fuel Proc. Tech. 89 (2008) 214-219.
- [11] B. Pietruszka, M. Heintze, Methane conversion at low temperature: the combined application of catalysis and non-equilibrium plasma; Cat. Today 90 (2004) 151–158
- [12] Istadi, N. A. S. Amin, Co-generation of synthesis gas and C₂C hydrocarbons from methane and carbon dioxide in a hybrid catalytic-plasma reactor: A review. Fuel 85 (2006) 577–592
- [13] E. El Ahmar, C. Met, O. Aubry, A. Khacef, J.M. Cormier, Hydrogen enrichment of a methane–air mixture by atmospheric pressure plasma for vehicle applications, Chem. Eng. J. 116 (2006) 13–18

- [14] X. Zhang, B. Wang, Y. Liu, G. Xu, Conversion of Methane by Steam Reforming Using Dielectric-barrier Discharge, *Chinese J. of Chem. Eng.*, (2009), 17(4) 625-629.
- [15] G.B. Zhao, S. John, J.J. Zhang, L. Wang, S. Muknahallipatna, J. C. Hamann, J.F. Ackerman, M. D. Argyle, O.A. Plum, Methane conversion in pulsed corona discharge reactors, *Chemical Engineering Journal* 125 (2006) 67–79
- [16] S. Kado, K. Urasaki, Y. Sekine, K. Fujimoto, Direct conversion of methane to acetylene or syngas at room temperature using non-equilibrium pulsed discharge, *Fuel* 82 (2003) 1377–1385.
- [17] Y. Chao, C.T. Huang, H.M. Lee, M.B. Chang, Hydrogen production via partial oxidation of methane with plasma-assisted catalysis, *Int. J. of Hydrogen Energy*, 33 (2008) 664 – 671.
- [18] B. Glocker, G. Nentwig, E. Messerschmid, 1-40 kW steam respectively multi gas thermal plasma torch system, *Vacuum* 59 (2000) 35-46
- [19] K. Shuzenji, T. Tachibana, Superiority of oxygen as feedstock for a plasma jet igniter in supersonic methane/air streams, *Proceedings of the Combustion Institute*, Volume 29, (2002) 875–881.
- [20] S.C. Kim, Y.N. Chun, Production of hydrogen by partial oxidation with thermal plasma *Renewable Energy* 33 (2008) 1564–1569
- [21] T. Lan, Y. Ran, H. Long, Y. Wang, Y. Yin, Experimental study on syngas production by carbon dioxide reforming of methane by plasma jet. *Natural Gas Industry*, 27, (2007) 129-32.
- [22] X. Tao, M. Bai, Q. Wu, Z. Huang, Y. Yin, X. Dai. CO₂ reforming of CH₄ by binode thermal plasma, *Int. J. of Hydrogen Energy*; 34(2009), 9373-9378.
- [23] Y.C. Yang, B.J. Lee, Y.N. Chun, Characteristics of methane reforming using gliding arc reactor, *Energy* 34 (2009) 172–177.
- [24] T. Sreethawong, P. Thakonpatthanakun, S. Chavadej, Partial oxidation of methane with air for synthesis gas production in a multistage gliding arc discharge system, *Int. J. of Hydrogen Energy* 32 (2007) 1067 – 1079.
- [25] Z. Bo, J. Yan, X. Li, Y. Chi, K. Cen, Plasma assisted dry methane reforming using gliding arc gas discharge: Effect of feed gases proportion, *Int. J. of Hydrogen Energy*, 33 (2008), 5545-5553
- [26] N. Rueangjitt, T. Sreethawong, S. Chavadej, H. Sekiguchi, Plasma-catalytic reforming of methane in AC micro-sized gliding arc discharge: Effects of input power, reactor thickness, and catalyst existence, *Chem. Eng. J.* 155 (2009) 874–880.
- [27] I.N. Kosarev, N.L. Aleksandrov, S.V. Kindysheva, S.M. Starikovskaia, A.Yu. Starikovskii, Kinetics of ignition of saturated hydrocarbons by nonequilibrium plasma: CH₄-containing mixtures, *Combustion and Flame*, 154 (2008) 569–586
- [28] D.P. Lymberopoulos, D.J. Economou, Fluid Simulations of glow discharges: Effect of metastable atoms in argon, *J. Appl. Phys.*; 73 (1993), 3668-3679
- [29] Y.J. Shiu, M.A. Biondi, Dissociative recombination in argon: Dependence of the total rate coefficient and excited-state production on electron temperature, *Phys. Rev. A*, 17, (1978), 868-872
- [30] C.M. Ferreira, J. Loureiro, Electron transport parameters and excitation rates in argon, *J. Phys D: Appl. Phys.* 16 (1983) 1611-1621
- [31] E.V. Karoulina, Y.A. Lebedev, Computer simulation of microwave and DC plasmas: Comparative characterization of plasmas, *J. Phys D: Appl. Phys* 25, (1992) 401-412
- [32] L.E. Kline, W.D. Partlow, W.E. Bies, Electron and chemical kinetics in methane rf glow-discharge deposition in plasmas, *J. Appl. Phys.*; 65 (1989), 70-78
- [33] A. Indarto, J.W. Choi, H. Lee, H.K. Song, Kinetic Modeling of Plasma Methane Conversion Using Gliding Arc, *Journal of Natural Gas Chemistry* 14 (2005), 13-21
- [34] H. R. Griem, *Principles of Plasma Spectroscopy*, Ed. Cambridge, (2005) p115,